Published in final edited form as:
Dev Neurobiol. 2012 September ; 72(9): 1243–1255. doi:10.1002/dneu.20990.

EphB signaling regulates target innervation in the developing and deafferented auditory brainstem

Paul A. Nakamura[1], **Candace Y. Hsieh**[1], and **Karina S. Cramer**[1,*]
[1]Department of Neurobiology & Behavior, University of California, Irvine, Irvine CA 92697

Abstract

Precision in auditory brainstem connectivity underlies sound localization. Cochlear activity is transmitted to the ventral cochlear nucleus (VCN) in the mammalian brainstem via the auditory nerve. VCN globular bushy cells project to the contralateral medial nucleus of the trapezoid body (MNTB), where specialized axons terminals, the calyces of Held, encapsulate MNTB principal neurons. The VCN-MNTB pathway is an essential component of the circuitry used to compute interaural intensity differences that are used for localizing sounds. When input from one ear is removed during early postnatal development, auditory brainstem circuitry displays robust anatomical plasticity. The molecular mechanisms that control the development of auditory brainstem circuitry and the developmental plasticity of these pathways are poorly understood. In this study we examined the role of EphB signaling in the development of the VCN-MNTB projection and in the reorganization of this pathway after unilateral deafferentation. We found that EphB2 and EphB3 reverse signaling are critical for the normal development of the projection from VCN to MNTB, but that successful circuit assembly most likely relies upon the coordinated function of many EphB proteins. We have also found that ephrin-B reverse signaling repels induced projections to the ipsilateral MNTB after unilateral deafferentation, suggesting that similar mechanisms regulate these two processes.

Keywords

EphB; ephrin-B; VCN; MNTB; deafferentation

INTRODUCTION

In the mammalian auditory brainstem, globular bushy neurons of the ventral cochlear nucleus (VCN) project to the contralateral, but not ipsilateral, medial nucleus of the trapezoid body (MNTB; Kuwabara et al., 1991), where they terminate in calyces of Held (Held, 1893). MNTB neurons provide inhibitory input to neurons in the adjacent lateral superior olive (LSO), which also receive tonotopically matched excitatory inputs from the ipsilateral VCN. In LSO neurons, the balance of inhibition from the contralateral side and excitation from the ipsilateral side aids in the computation of interaural level differences used for sound localization (Cant and Casseday, 1986; Sanes, 1990; Glendenning et al., 1992). Accurate detection of these differences relies on the precise wiring of auditory brainstem circuitry. The VCN-MNTB projection is established during embryonic and postnatal development, and VCN axons appear to project directly to contralateral MNTB, without making transient ipsilateral connections (Kil et al., 1995; Nakamura and Cramer, 2010).

[*]**Corresponding Author:** Department of Neurobiology and Behavior, University of California, Irvine, 2205 McGaugh Hall, Irvine, CA 92697-4550, cramerk@uci.edu.

Previous studies have shown that Eph signaling has significant roles in the development of the avian and mammalian auditory brainstem (Cramer, 2005; Nakamura and Cramer, 2010). Eph proteins, Eph receptors and ephrin ligands, mediate cell-cell bidirectional signaling; upon binding, forward signaling acts through Eph receptors in the Eph-expressing cell while reverse signaling acts through ephrins in the ephrin-expressing cell. Interactions between Ephs and ephrins can result in attraction or repulsion. Eph proteins are divided into A and B subclasses. EphA's preferentially bind to ephrin-A's and EphB's preferentially bind to ephrin-B's, with a few exceptions (Flanagan and Vanderhaeghen, 1998; Kullander and Klein, 2002). Notably, EphA4 binds to ephrin-B2 (Gale et al., 1996) and EphB2 binds to ephrin-A5 (Himanen et al., 2004). We previously showed that mutant mice with reduced ephrin-B reverse signaling display a significant number of projections from VCN to ipsilateral MNTB (Hsieh et al., 2010), suggesting that this signaling normally prevents the formation of ipsilateral calyces. We observed abnormal MNTB targeting in two separate lines of mice, one with decreased reverse signaling through ephrin-B2 and another with null mutations in *EphB2* and *EphB3*, both receptors for the ephrin-B2 ligand. However, the large number of possible binding interactions presents a challenge for determining how Eph signaling is integrated to generate precise projections during development.

An understanding of the regulation of VCN-MNTB projections can be further informed by lesion studies. After unilateral removal of the cochlea, VCN neurons on the lesioned side undergo cell death (Hashisaki and Rubel, 1989; Mostafapour et al., 2000), while axons from the intact VCN branch and produce novel calyceal projections to the ipsilateral MNTB (Kitzes et al., 1995; Russell and Moore, 1995; Hsieh et al., 2007). An interesting possibility is that lesion-induced reorganization shares mechanisms that control normal development.

In this study we characterized the spatiotemporal expression patterns of all EphB receptors and their binding partners in the VCN-MNTB pathway during embryonic and postnatal development. These expression patterns suggest that EphB signaling influences VCN axon guidance during several stages of VCN-MNTB circuit formation at various ages. To further understand the role of EphB signaling, we tested which EphB receptors act to restrict VCN-MNTB projections during normal development. We found that *EphB2*;*EphB3* double mutants show significant ipsilateral VCN-MNTB projections, whereas single mutations showed no effect. Finally, we tested whether EphB signaling regulates reorganization after cochlea removal. We found that significantly greater lesion-induced ipsilateral projections are induced in EphB mutants than in wild type mice. These findings suggest that the molecular mechanisms underlying specificity in normal development are similarly operative during lesion-induced synaptogenesis.

METHODS

Mice

All procedures were approved by the University of California, Irvine Institutional Animal Care and Use Committee. Wild type, *EphB2*^{null}, *EphB3*^{null}, *EphB2*^{null};*EphB3*^{null}, *EphB2*^{lacZ};*EphB3*^{null}, and *ephrin-B2*^{lacZ} mutant mouse lines (Fig. 1) on a mixed CD-1/129 background were used in this study. The *EphB2*^{null} line lacks the entire EphB2 protein; there is no EphB2 forward signaling and no EphB2-elicited ephrin-B reverse signaling (Fig. 1B; Henkemeyer et al., 1996). Similarly, the *EphB3*^{null} mouse line lacks forward and reverse signaling via EphB3 (Fig. 1C; Henkemeyer et al., 1996). The *EphB2*^{null};*EphB3*^{null} compound mutant line lacks EphB2 and EphB3 forward signaling and EphB2- and EphB3-induced reverse signaling (Fig. 1D). The *EphB2*^{lacZ};*EphB3*^{null} mutant mouse line has the extracellular, transmembrane, and juxtamembrane domains of EphB2 fused to β–galactosidase intracellularly and a null mutation in *EphB3*; this allows for normal EphB2-induced ephrin-B reverse signaling, but no forward signaling through EphB2 and EphB3

(Fig. 1E; Henkemeyer et al., 1996). The *Ephrin-B2*^{lacZ} line has an allele that encodes the extracellular domain of ephrin-B2 fused to an intracellular β–galactosidase, which results in reduced ephrin-B2 reverse signaling, but intact ephrin-B2-elicited forward signaling (Fig. 1F; Dravis et al., 2004). Because *ephrin-B2*^{lacZ} homozygous mutants die perinatally (Cowan et al., 2004), only *ephrin-B2*^{lacZ} heterozygous mutants were used in this study. We used mice from ages embryonic day 13.5 (E13.5) to postnatal day 5 (P5), with E0.5 set as noon on the day the vaginal plug was found and P0 being the day of birth. Mice were genotyped with PCR using DNA obtained from tail samples. Primer sequences for PCR and PCR product sizes have been described previously (Henkemeyer et al., 1996; Dravis et al., 2004; Hsieh et al., 2010). None of the mutant mice used in this study are deaf (Howard et al., 2003; Miko et al., 2007; Miko et al., 2008).

Immunohistochemistry

For embryonic ages, tissue was immersion fixed for 1 hour in 4% paraformaldehyde (PFA) in phosphate buffered saline (PBS) at 4°C and then cryoprotected in 30% sucrose in PBS overnight at 4°C. For postnatal ages, pups were euthanized with isoflurane and transcardially perfused with 0.9% saline then 4% PFA in PBS. Brainstems were removed and postfixed for 1 hour in 4% PFA in PBS at 4°C and then cryoprotected in 30% sucrose in PBS at 4°C overnight. For all ages, coronal sections were cut on a cryostat (Leica Microsystems) at 18–20 μm and mounted directly onto chrome-alum-subbed slides. Slides were rinsed in 0.1 M Tris-buffered saline (pH 7.4; TBS) and then incubated in 0.03% H_2O_2 in methanol for 10 minutes, rinsed in 0.05% Triton X-100 in TBS (TBST), and then immersed in blocking solution containing 3% normal serum in TBST for 1 hour. After blocking, slides were briefly rinsed in TBST and then incubated overnight in primary antibody in 1% serum in TBST. The following day, slides were rinsed in TBS, incubated with a biotinylated secondary antibody, either goat anti-rabbit, goat anti-mouse, or rabbit anti-goat (6 μg/ml, Vector Laboratories), in 1% serum in TBST for 2 hours, rinsed with TBS, and then incubated in ABC solution (Vector Laboratories) for 1 hour. Slides were then rinsed with TBS and reacted with 3,3'-diaminobenzidine, rinsed, dehydrated in a graded series of ethanol to xylenes, and coverslipped with DPX mountant (VWR International). The following primary antibodies were used: rabbit anti-ephrin-B1 (5 μg/ml, Invitrogen), goat anti-ephrin-B2 (10 μg/ml, Neuromics), rabbit anti-ephrin-B3 (5 μg/ml, Invitrogen), rabbit anti-ephrin-A5 (5 μg/ml, Invitrogen), mouse anti-EphB1-3 (1 μg/ml, Developmental Studies Hybridoma Bank), rabbit anti-EphB2 (5 μg/ml, Invitrogen), rabbit anti-EphB3 (5 μg/ml, Abcam), mouse anti-EphB4 (5 μg/ml, Invitrogen), and mouse anti-EphB6 (5 μg/ml, Abcam). In a subset of embryonic animals, we used MafB immunohistochemistry (0.1 μg/ml, Santa Cruz Biotechnology) in parallel sections to confirm the location of the cochlear nucleus (Howell et al., 2007).

The ephrin-B1 antibody was generated against the internal sequence of mouse ephrin-B1 (aa 150–240 of P52795). Western blot analysis yielded a single band at 50 kDa. The ephrin-B2 antibody was generated against the extracellular domain of ephrin-B2 (aa 27–227 of AAA8293) and produces a main, single band at ~40 kDa (Migani et al., 2007). The ephrin-B3 antibody binds to the internal sequence of ephrin-B3 (aa 165–250 of NP_031937) and yielded a single band at 55 kDa on a western blot. The ephrin-A5 antibody was generated against the C-terminal end of mouse ephrin-A5 (aa 160–250) and produces a band at ~25 kDa on a western blot (manufacturer's technical information). The EphB1-3 antibody was generated using recombinant rat EphB1 protein (aa 18–538). On western blots, this antibody recognizes EphB1, EphB3, and weakly binds to EphB2, but not to EphB4 or EphB6 (Jevince et al., 2006). The EphB2 antibody binds to the juxtamembrane region of EphB2 (aa 530–615 of NP_034272) and produced a single band at 120 kDa on western blot. The EphB3 antibody was generated using recombinant human EphB3 (NP_004434) and yields a single

band at 110 kDA on western blots with mouse tissue (manufacturer's technical information). The EphB4 antibody (clone 3D7G8) was generated using a recombinant protein derived from the C-terminal region of EphB4 and on western blots it identifies a single band at ~115 kDa (manufacturer's technical information). The EphB6 antibody was generated using a recombinant protein corresponding to aa 23–122 of human EphB6 and yields a single band of 109 kDa on western blots (manufacturer's technical information).

Neuroanatomical labeling

Mice were euthanized with an overdose of isoflurane and then perfused transcardially with 0.9% saline followed by 4% PFA in PBS. Brainstems were extracted and following post-fixation overnight in 4% PFA in PBS at 4°C, the cerebellum was dissected away and a small piece (100–200 μm^2) of NeuroVue Red dye (PTI Research) was inserted into VCN (Hsieh et al., 2007; Hsieh et al., 2010). The brainstems were then returned to 4% PFA in PBS and incubated at 37°C for 2–3 weeks to allow for dye transport. Coronal brainstem sections were cut at 100 μm on a vibratome (Leica Microsystems), mounted onto chrome-alum-subbed slides, and coverslipped with Glycergel mounting media (Dako). Labeling was performed at P10-12 for studies of normal development, and at P9-11 for studies of deafferentation-induced plasticity.

Cochlea removal

Unilateral cochlea removals (CR) were performed at P2–P3 as previously described (Hsieh and Cramer, 2006; Hsieh et al., 2007). Mouse pups were anesthetized with hypothermia and an incision was made ventral to the pinna to expose the tympanic membrane. Using a sterile pipette, the middle ear mesenchyme and ossicles were aspirated and then the pipette was inserted into the oval window to aspirate the cochlea. The procedure was performed with a stereomicroscope using heat-sterilized instruments (Germinator 500, CellPoint Scientific). Following the surgery, pups were warmed on a heating pad and then returned to their home cage with their mothers for 7–8 days. After this survival period, the pups were sacrificed and the VCN-MNTB projection was labeled using the neuroanatomical labeling procedure described above.

Imaging

Brainstem sections were examined, analyzed, and digitally imaged with a Zeiss Axioskop microscope, Axiocam camera, and Openlab software (Improvision). High-powered images were acquired as three-dimensional stacks on a custom-built two photon laser-scanning microscope using Slidebook software (Intelligent Imaging Innovations, Inc). Digital images were imported into Adobe Photoshop to adjust brightness and contrast and then imported into Adobe Illustrator for photomicrograph production.

Data analysis

To determine the specificity of the VCN-MNTB projection in mutant mice during normal development and to compare the amount of deafferentation-induced sprouting to MNTB between our different lines of mutant mice, we counted all labeled calyceal terminations in MNTB on both sides and calculated an ipsilateral to contralateral (I/C) ratio for each mouse as described previously (Hsieh and Cramer, 2006; Hsieh et al., 2007; Hsieh et al., 2010). Briefly, we counted the dye-labeled calyces in the MNTB ipsilateral to the VCN with the dye placement and divided this number by the total number of calyces counted in the MNTB contralateral to the dye-injected VCN to normalize for differences in the amount of dye used between animals. A termination was counted as a calyx if at least one-third of the MNTB cell surface was covered. All counts were performed blind to genotype. We used a Wilcoxon/Kruskal-Wallis rank-sum test to determine differences in I/C ratios between

groups of different genotypes. For the parametric two-way ANOVA, we transformed the I/C ratio data using an arcsine transformation and compared these data to transformed I/C ratios obtained from non-operated, age-matched controls of the same genotype.

To determine if genotype had an effect on the degree of VCN degeneration following CR, we measured the volume of VCN on the lesioned and intact sides and divided the lesioned VCN volume by the intact VCN volume to calculate a percentage of remaining VCN for each animal in a random subset of animals. For measuring the volume of VCN, we measured the area of VCN in every other section containing VCN using Openlab software, multiplied the summed areas by 2 (the section spacing), and then by 100 μm (the section thickness). All measurements of VCN volume were performed blind to genotype. We then grouped the animals by genotype and compared means with an ANOVA.

RESULTS

Several EphB proteins are expressed during VCN-MNTB development

Because there are several proteins in the EphB subfamily with broad binding specificity, we examined the expression of all ephrin-B ligands and EphB receptors at embryonic day 13.5 (E13.5), when VCN axons are crossing the midline to reach the contralateral MNTB (Howell et al., 2007), at E17.5, when VCN axons first contact contralateral MNTB neurons (Hoffpauir et al., 2010), and at postnatal day 0 (P0) and P4-5, during calyx of Held formation and maturation (Kil et al., 1995; Hoffpauir et al., 2006; Nakamura and Cramer, 2010). In order to understand EphB signaling during VCN-MNTB development, we documented the spatiotemporal expression of EphB1, EphB2, EphB3, EphB4, and EphB6, as well as that of their binding partners, ephrin-B1, ephrin-B2, ephrin-B3, and ephrin-A5 ($n \geq 3$ mice for each antibody at every age).

Embryonic development—At E13.5, when VCN axons are crossing the midline to innervate the contralateral MNTB, we observed expression of ephrin-B2 (Fig. 2A), ephrin-B3 (Fig. 2B), ephrin-A5 (Fig. 2C), EphB2 (Fig. 2D), and EphB4 (Fig. 2E) in the cochlear nucleus (asterisks in Fig. 2A–E). Many EphB proteins were also expressed at the midline (arrowheads in Fig. 2F–L) of the auditory brainstem. Ephrin-B2 (Fig. 2F), ephrin-B3 (Fig. 2G), and all EphB receptors (Fig. 2H–L) were present at the midline at varying levels, with ephrin-B3 expressed the most. We did not observe any EphB staining in VCN axons and MNTB is not identifiable at this age.

At E17.5, when MNTB neurons are first innervated by VCN axons (Hoffpauir et al., 2010), ephrin-B1 (Fig. 3A), ephrin-B2 (Fig. 3B), ephrin-A5 (Fig. 3C), and EphB1, 2, and 3 (Fig. 3D–E) were expressed in the VCN (asterisks in Fig. 3A–E). Similar to the observations in E13.5 brainstems, ephrin-B2 (Fig. 3F), ephrin-B3 (Fig. 3G), and all EphB receptors (Fig. 3H–L) were expressed at the midline (arrowheads in Fig. 3F–L) at this age, with heaviest staining of ephrin-B3. We did not observe any staining in VCN axons or in MNTB neurons at E17.5.

Postnatal development—Expression of ephrin-B's and EphB's was evident in VCN axons and MNTB neurons at P0. Ephrin-B1 (Fig. 4A), ephrin-B2 (Fig. 4B), ephrin-A5 (Fig. 4C), and EphB1, 2, and 3 (Fig. 4D) were expressed in VCN (asterisks in Fig. 4A–D) and ephrin-B1 (Fig. 5A) and EphB2 (Fig. 5B) expression was evident in VCN axons. Ephrin-B1 (Fig. 5A), ephrin-A5 (Fig. 5C), and EphB3 (Fig. 5D) were expressed in MNTB. Ephrin-B2 (Fig. 5E), ephrin-B3 (Fig. 5F), and EphB3 (Fig. 5G) were expressed at the midline (arrowheads in Fig. 5E–G) of the brainstem at this age, while the expression of all other EphB receptors was no longer detectable in this region.

Similar to expression at P0, ephrin-B1 (Fig. 4E), ephrin-B2 (Fig. 4F), ephrin-A5 (Fig. 4G), and EphB1, 2, and 3 (Fig. 4H) were present in VCN (asterisks in Fig. 4E–H) and ephrin-B1 (Fig. 6A) and EphB2 (Fig. 6B) were expressed in VCN axons at P4-5. However, the expression of ephrin-B2 in MNTB neurons (Fig. 6C), in addition to ephrin-B1 (Fig. 6A), ephrin-A5 (Fig. 6D), and EphB3 (Fig. 6E), became evident by this age. The expression of EphB3 in MNTB at P4 appeared less than at P0. At P4-5, the only Eph protein expressed at the midline (arrowhead in Fig. 6F) of the auditory brainstem was ephrin-B3 (Fig. 6F). Expression results are summarized in Table 1.

EphB2 and EphB3 reverse signaling is required for normal development

We have previously shown that *EphB2*^{null};*EphB3*^{null}, but not *EphB2*^{lacZ};*EphB3*^{null}, double mutant mice have aberrant projections to the ipsilateral MNTB (Hsieh et al., 2010). However, it is unclear whether EphB2 alone or EphB2 and EphB3 together are necessary for the ephrin-B reverse signaling required to restrict the VCN projections to the contralateral MNTB. To address this question, we traced the VCN-MNTB pathway in P10–P12 wild type and *EphB2*^{null} single mutant mice and compared the I/C ratios to those obtained from *EphB3*^{null} single mutant mice and *EphB2*^{null};*EphB3*^{null} double mutant mice (Hsieh et al., 2010). Similar to wild type mice, *EphB2*$^{-/-}$ mice had projections from VCN that terminated almost exclusively in the contralateral MNTB (Fig. 7). An example of labeling can be seen in Fig. 7B, where calyces can be seen in the contralateral MNTB (high-powered image in inset), but not in the ispilateral MNTB. Wild type and *EphB2*$^{-/-}$ mutant mice had mean I/C ratios of 0.03 ± 0.01 (n=9) and 0.03 ± 0.01 (n=7), respectively, which did not differ from each other (P = 0.87) and from *EphB3*$^{-/-}$ mutant mice (P = 0.40 and 0.30; Fig. 7A), which had a mean I/C of 0.03 ± 0.01 (n=14). *EphB2*$^{-/-}$;*EphB3*$^{-/-}$ mice had a mean I/C ratio of 0.14 ± 0.03 (n=5), which is greater than wild type (P < 0.05), *EphB2*$^{-/-}$ (P < 0.05), and *EphB3*$^{-/-}$ mutant mice (P < 0.05; Fig. 7A). These data suggest that EphB2 and EphB3 have an overlapping function in regards to the normal development of the VCN-MNTB projection; in the absence of either EphB2 or EphB3, the other can compensate for this loss.

EphB signaling regulates the induced projection from VCN to the ipsilateral MNTB

Because signaling between EphB proteins plays a role in the normal development of the VCN-MNTB pathway, we asked whether this signaling also plays a role in the formation of the projection from VCN to the ipsilateral MNTB induced by early unilateral deafferentation, when this circuit is still maturing. To determine if EphB signaling also influences the induced projection to MNTB from the ipsilateral VCN, we unilaterally removed the cochlea at P2-3 in wild type, *ephrin-B2*^{lacZ}, *EphB2*^{null};*EphB3*^{null}, and *EphB2*^{lacZ};*EphB3*^{null} mutant mice, labeled the VCN-MNTB pathways after a survival period of 7–8 days, which is sufficient to permit formation of lesion-induced ipsilateral projections (Hsieh and Cramer, 2006), and compared I/C ratios between genotypes. In all genotypes we observed a substantial projection to the ipsilateral MNTB after unilateral deafferentation (Fig. 8). After cochlea removal (CR), wild type mice had a mean I/C ratio of 0.23 ± 0.04 (n = 14; Fig. 8A and 8B). *Ephrin-B2*$^{lacZ/+}$ mice had a mean I/C ratio of 0.37 ± 0.07 (n=10; Fig. 8A and 8C), which was greater than the mean obtained from wild type mice (P < 0.05). *EphB2*$^{-/-}$;*EphB3*$^{-/-}$ mice had a mean I/C ratio of 0.44 ± 0.03 (n = 4; Fig. 8A and 8D), which was also greater than the mean I/C ratio of wild type mice (P < 0.05) after unilateral deafferentation. In contrast, CR in *EphB2*$^{lacZ/lacZ}$;*EphB3*$^{-/-}$ mice resulted in a mean I/C ratio of 0.18 ± 0.06 (n=5; Fig. 8A and 8E), which did not differ from the wild type mean I/C ratio (P = 0.40) and suggests that EphB2 forward signaling does not affect this process.

Two distinct possibilities could account for the increased I/C ratios in *ephrin-B2*$^{lacZ/+}$ and *EphB2*$^{-/-}$;*EphB3*$^{-/-}$ mice after unilateral deafferentation. One possibility is that they had

more induced sprouting to the ipsilateral MNTB. An alternative explanation is that they had higher I/C ratios than wild type mice before surgery (Hsieh et al., 2010), but the amount of induced sprouting was not any more than the amount of sprouting observed in wild types. To address these two possibilities, we performed a two-way ANOVA on arcsine-transformed I/C ratios, with genotype (wild type or mutant) and surgical status (non-operated or CR) as independent factors. We found that in *ephrin-B2*$^{lacZ/+}$ mice, the amount of induced projections to the ipsilateral MNTB did not differ from wild type ($P = 0.90$, genotype-surgical status interaction; Fig. 8F). Similarly, the level of induced sprouting to the ipsilateral MNTB in *EphB2*$^{-/-}$;*EphB3*$^{-/-}$ mice was not greater than the level observed in wild type mice ($P = 0.60$, genotype-surgical status interaction; Fig 8G), providing evidence to support the latter possibility.

However, because *ephrin-B2*$^{lacZ/+}$ and *EphB2*$^{-/-}$;*EphB3*$^{-/-}$ mice have a substantial projection to the ipsilateral MNTB without surgery (about 15% of MNTB neurons receive input from the ipsilateral VCN (Hsieh et al., 2010)), it is expected that following unilateral deafferentation, the denervated MNTB in these mutant mice lose less inputs compared to wild type mice (in which only about 3% of MNTB neurons receive input from the ipsilateral VCN). With fewer MNTB neurons to re-innervate and less drive for axonal sprouting after unilateral deafferentation, an *equal* amount of induced sprouting would actually indicate *more* plasticity in *ephrin-B2*$^{lacZ/+}$ and *EphB2*$^{-/-}$;*EphB3*$^{-/-}$ mice. For a more direct comparison, we performed unilateral CR in *EphB2*$^{-/-}$ and *EphB3*$^{-/-}$ single mutant mice, mice in which the level of MNTB innervation by the ipsilateral VCN does not differ from wild type mice (Fig. 7) and the amount of MNTB denervation following CR would be the same as the level in wild type mice. Interestingly, we found that *EphB2*$^{-/-}$ and *EphB3*$^{-/-}$ mice had mean I/C ratios of 0.38 ± 0.05 ($n = 6$; Fig. 8A and 8H) and 0.18 ± 0.03 ($n = 8$; Fig. 8A and 8I), respectively, after unilateral deafferentation. This mean I/C ratio from *EphB2*$^{-/-}$ mice was greater than the mean I/C ratio obtained in wild type mice ($P < 0.05$), but did not differ from the ratios of *ephrin-B2*$^{lacZ/+}$ ($P = 0.59$) and *EphB2*$^{-/-}$;*EphB3*$^{-/-}$ mice ($P = 0.52$). The mean *EphB3*$^{-/-}$ I/C ratio after CR was not different from the mean wild type I/C ratio after CR ($P = 0.49$).

To confirm that the differences in I/C ratios were due to differences in the amount of sprouting to MNTB and not from differences in the degree of VCN degeneration caused by CR, we compared the extent of VCN degeneration between wild type and *EphB2*$^{lacZ/lacZ}$;*EphB3*$^{-/-}$ mutants, mice in which the mean I/C ratios did not differ from the mean wild type I/C ratio, and *EphB2*$^{-/-}$ mutants, mice in which the mean I/C ratio was greater than the mean I/C ratio of wild types. After unilateral CR, we found that in wild type, *EphB2*$^{lacZ/lacZ}$;*EphB3*$^{-/-}$, and *EphB2*$^{-/-}$ mice the mean percentages of VCN remaining was 22.27 ± 2.27, 30.92 ± 9.47, and 27.61 ± 11.72, respectively. These means did not differ from each other ($P = 0.79$; $n = 3$ animals for each genotype), suggesting that genotype does not affect the amount of VCN cell death after CR.

DISCUSSION

We previously found that compound null mutations in *EphB2* and *EphB3* reduce precision in contralateral VCN-MNTB pathway targeting (Hsieh et al., 2010). Here, we explored the mechanisms by which EphB signaling regulates targeting in this pathway. We first performed a comprehensive spatiotemporal expression study of all ephrin-B's and EphB's and found that multiple ephrin-B ligands and EphB receptors are expressed in this pathway at various stages of development. We then determined that the compound mutation is needed for the observed phenotype, as single mutations in *EphB2* or *EphB3* do not show this effect. Together with our previous study, these results suggest that ephrin-B reverse signaling regulates contralateral VCN-MNTB targeting, and that precision in this pathway

results from coordinated function of several EphB proteins. Finally, we investigated the role of EphB signaling in lesion-induced ipsilateral projections. We examined the VCN-MNTB pathway in EphB mutant and wild type mice after cochlea removal during early postnatal development, when this circuit is relatively immature (Rodriguez-Contreras et al., 2008; Rusu and Borst, 2011). Our results suggest that EphB reverse signaling also limits innervation of the ipsilateral MNTB after early postnatal deafferentation, similar to the regulation of ipsilateral MNTB innervation during normal development. However, unlike normal development, this ephrin-B2 reverse signaling seems to be mostly elicited by EphB2 alone and does not appear to be compensated by EphB3.

EphB signaling in *trans* vs. *cis*

Brainstem regions with immunolabeling expressed both ephrin-B ligands and EphB receptors. Ephrins and Eph receptors expressed in the same cell can interact in a *cis* fashion, which is believed to block *trans* interactions (Hornberger et al., 1999; Carvalho et al., 2006) and may thus play a role in the development of this pathway. For example, ephrin-B2, which shows increased expression in MNTB at P4, could bind to EphB3 within MNTB neurons. This binding would reduce the level of EphB3 available to bind to ephrin-B1 expressed in VCN axons, and could consequently reduce repulsion. Co-expressed EphB2 and ephrin-B1 could similarly interact in VCN axons.

Innervation of contralateral vs. ipsilateral targets

Our data suggest that the regulation of contralateral vs. ipsilateral targeting in the VCN-MNTB pathway depends on two key points, one at the midline and the other within MNTB. Our expression studies suggest that EphB signaling between growing axons and the midline is limited at early ages. At E13.5, when VCN axons cross the midline (Howell et al., 2007), we observed minimal levels of EphB and ephrin-B expression in these axons. Midline expression was heavy at this age and did not start to decrease until P4. Low expression of EphB proteins in VCN axons may permit midline crossing at this age. In the chick auditory brainstem, ephrin-B2-expressing cochlear nucleus axons cross the midline when EphB expression in this region is very low, and EphB2 is up-regulated at the midline after these axons cross. Additionally, EphB2 misexpression at the midline dramatically increases axon misrouting, suggesting that midline EphB receptors inhibit cochlear nucleus axons (Cramer et al., 2006). It is possible that in the chick auditory brainstem, EphB expression at the midline creates a repulsive barrier, which prevents the re-crossing of cochlear nucleus axons. Unlike this developmental sequence in chicks, in this study we observed heavy expression at the midline at the time when VCN axons cross, and little expression in VCN axons until P0, well after midline crossing.

In the mouse auditory brainstem, it is not clear to what extent EphB signaling influences the initial growth of axons across the midline. EphB proteins may prevent axon growth, but only after expression emerges in axons. The delay from axon crossing to onset of axonal EphB expression contrasts with that seen in other areas of the central nervous system. For example, in the mouse spinal cord, ephrin-B3 at the midline controls the crossing of EphB- and EphA4-positive commissural axons (Kullander et al., 2001; Yokoyama et al., 2001; Kadison et al., 2006). Additionally, at the mouse optic chiasm, ephrin-B2 in midline glial cells repulse EphB1-expressing retinal ganglion cell axons into the ipsilateral optic tract (Petros et al., 2009).

EphB signaling may thus be limited in its control of initial midline crossing. Consistent with this prediction, in EphB mutant mice we found that most VCN-MNTB axons cross the midline and form appropriate contralateral projections. However, a proportion of the observed ipsilateral projections appear to emerge from VCN axons that did not reach the

midline, indicating a defect in midline guidance (Hsieh et al., 2010). Mutations in other axons guidance molecules such as netrins, DCC, slits, and robos show stronger effects in which the entire VCN-MNTB projection fails to reach the midline (Howell et al., 2007; Renier et al., 2010). These data suggest that Eph-ephrin interactions work in conjunction with other axon guidance molecules that provide strong attractive cues for the initial growth to the midline.

Expression of EphB proteins at the midline may differentially influence the response of EphB-positive axons in contraleral vs. ipsilateral targets. For example, EphB2 in VCN axons may respond differently to ephrin-B2 and/or ephrin-A5 in the contralateral MNTB after interacting with ephrin-B2 and -B3 at the midline, an instance where EphB2 signaling might be repulsive in the ipsilateral target, but attractive in the contralateral target. A potential molecular mechanism that could mediate the repulsiveness vs. attractiveness of EphB interactions is EphB-ephrin-B endocytosis, (Zimmer et al., 2003), which could occur at the midline, creating opposing effects of EphB signaling on different sides of the brainstem.

The distribution of EphB proteins in VCN neurons may differ in the proximal and distal regions of axons, creating distinct molecular environments and different interactions for the ipsilateral and contralateral MNTB. EphB-ephrin-B interactions may be more prominent in the ipsilateral MNTB if diffusion of EphB transcript or protein is limited. In the visual system, the response of Eph-expressing retinal axons depends on the concentration of ephrins, where high concentrations are repulsive and low concentrations are attractive (Hansen et al., 2004). Conversely, EphB expression could be up-regulated at the midline (Brittis et al., 2002), which could enable asymmetric EphB signaling between the ipsilateral and contralateral MNTB.

Aberrant innervation of the ipsilateral MNTB in *EphB2*^{null};*EphB3*^{null} double mutant mice during normal development may arise from multiple mechanisms at these two points, the midline and the MNTB. Our data showing the decline in EphB3 expression at early postnatal ages suggest that EphB3 signaling may be relatively more important for limiting ipsilateral projections during initial axon growth in the embryonic ages, while EphB2, which shows a more prolonged expression pattern, may regulate both early and late developmental events. This difference between EphB2 and EphB3 function is supported by our CR data in postnatal single mutant mice. The *EphB2* mutation shows an increase in lesion-induced ipsilateral projections, while the *EphB3* mutation does not, consistent with the observation that *EphB3* expression has decreased by the time of that lesions were performed at P2-3. These CR data, along with our observations in *ephrin-B2*^{lacZ} mice during normal development (Hsieh et al., 2010), support the idea of different roles for EphB2 and EphB3 and the role of ephrin-B2 reverse signaling as an effector for EphB functions in axon guidance and targeting.

EphB signaling during normal development and developmental plasticity

In this study, we have found that mutations in EphB proteins that affect normal development also affect developmental plasticity. Chemorepulsive molecules expressed at the time of lesion may have a similar inhibitory function during axonal reorganization after lesion. While it is possible that deafferentation alters the levels of Eph proteins, it seems unlikely based on previously reported work. The amount of lesion-induced sprouting due to a null mutation in *EphA4* was greater than what we observed in EphB mutant mice; however, there was no change in the level of EphA4 expression after unilateral deafferentation (Hsieh et al., 2007). Furthermore, this null mutation in *EphA4* does not affect normal development, but only the extent of induced ipsilateral innervation after unilateral deafferentation. However, it may be that EphA4 signaling does have a role during normal development of the VCN-MNTB projection, but that other EphA receptors can compensate when only EphA4 is

removed. Indeed, we have not observed any aberrant VCN-MNTB phenotypes during development in single EphB receptor mutant mice. Because EphA4 binds to ephrin-B2 (Gale et al., 1996), it is possible that the effect observed in the *EphA4* null mouse after unilateral deafferentation is due to reduced ephrin-B reverse signaling. Moreover, the reactivity between EphA4 and both ephrin-A's and ephrin-B's suggests that there may be cooperative interactions between these classes during the maturation of auditory system circuitry (Miko et al., 2007; Miko et al., 2008; Gabriele et al., 2011).

Acknowledgments

This work was supported by grants NIH F31DC010092, NIH P30DC008369, and NSF IOS-0642346. The authors are grateful to Dr. Mark Henkemeyer for providing transgenic mice and to Minhan Dinh for helpful comments on the manuscript.

REFERENCES

Brittis PA, Lu Q, Flanagan JG. Axonal protein synthesis provides a mechanism for localized regulation at an intermediate target. Cell. 2002; 110:223–235. [PubMed: 12150930]

Cant NB, Casseday JH. Projections from the anteroventral cochlear nucleus to the lateral and medial superior olivary nuclei. J Comp Neurol. 1986; 247:457–476. [PubMed: 3722446]

Carvalho RF, Beutler M, Marler KJ, Knoll B, Becker-Barroso E, Heintzmann R, Ng T, Drescher U. Silencing of EphA3 through a cis interaction with ephrinA5. Nat Neurosci. 2006; 9:322–330. [PubMed: 16491080]

Cowan CA, Yokoyama N, Saxena A, Chumley MJ, Silvany RE, Baker LA, Srivastava D, Henkemeyer M. Ephrin-B2 reverse signaling is required for axon pathfinding and cardiac valve formation but not early vascular development. Dev Biol. 2004; 271:263–271. [PubMed: 15223333]

Cramer KS. Eph proteins and the assembly of auditory circuits. Hear Res. 2005; 206:42–51. [PubMed: 16080997]

Cramer KS, Cerretti DP, Siddiqui SA. EphB2 regulates axonal growth at the midline in the developing auditory brainstem. Dev Biol. 2006; 295:76–89. [PubMed: 16626680]

Dravis C, Yokoyama N, Chumley MJ, Cowan CA, Silvany RE, Shay J, Baker LA, Henkemeyer M. Bidirectional signaling mediated by ephrin-B2 and EphB2 controls urorectal development. Dev Biol. 2004; 271:272–290. [PubMed: 15223334]

Flanagan JG, Vanderhaeghen P. The ephrins and Eph receptors in neural development. Annu Rev Neurosci. 1998; 21:309–345. [PubMed: 9530499]

Gabriele ML, Brubaker DQ, Chamberlain KA, Kross KM, Simpson NS, Kavianpour SM. EphA4 and ephrin-B2 expression patterns during inferior colliculus projection shaping prior to experience. Dev Neurobiol. 2011; 71:182–199. [PubMed: 20886601]

Gale NW, Holland SJ, Valenzuela DM, Flenniken A, Pan L, Ryan TE, Henkemeyer M, Strebhardt K, Hirai H, Wilkinson DG, Pawson T, Davis S, Yancopoulos GD. Eph receptors and ligands comprise two major specificity subclasses and are reciprocally compartmentalized during embryogenesis. Neuron. 1996; 17:9–19. [PubMed: 8755474]

Glendenning KK, Baker BN, Hutson KA, Masterton RB. Acoustic chiasm V: inhibition and excitation in the ipsilateral and contralateral projections of LSO. J Comp Neurol. 1992; 319:100–122. [PubMed: 1317390]

Hansen MJ, Dallal GE, Flanagan JG. Retinal axon response to ephrin-as shows a graded, concentration-dependent transition from growth promotion to inhibition. Neuron. 2004; 42:717–730. [PubMed: 15182713]

Hashisaki GT, Rubel EW. Effects of unilateral cochlea removal on anteroventral cochlear nucleus neurons in developing gerbils. J Comp Neurol. 1989; 283:5–73. [PubMed: 2745749]

Held H. Die zentrale Gehörleitung. Arch Anat Physiol Anat Abtheil. 1893; 17:201–248.

Henkemeyer M, Orioli D, Henderson JT, Saxton TM, Roder J, Pawson T, Klein R. Nuk controls pathfinding of commissural axons in the mammalian central nervous system. Cell. 1996; 86:35–46. [PubMed: 8689685]

Himanen JP, Chumley MJ, Lackmann M, Li C, Barton WA, Jeffrey PD, Vearing C, Geleick D, Feldheim DA, Boyd AW, Henkemeyer M, Nikolov DB. Repelling class discrimination: ephrin-A5 binds to and activates EphB2 receptor signaling. Nat Neurosci. 2004; 7:501–509. [PubMed: 15107857]

Hoffpauir BK, Grimes JL, Mathers PH, Spirou GA. Synaptogenesis of the calyx of Held: rapid onset of function and one-to-one morphological innervation. J Neurosci. 2006; 26:5511–5523. [PubMed: 16707803]

Hoffpauir BK, Kolson DR, Mathers PH, Spirou GA. Maturation of synaptic partners: functional phenotype and synaptic organization tuned in synchrony. J Physiol. 2010; 588:4365–4385. [PubMed: 20855433]

Hornberger MR, Dutting D, Ciossek T, Yamada T, Handwerker C, Lang S, Weth F, Huf J, Wessel R, Logan C, Tanaka H, Drescher U. Modulation of EphA receptor function by coexpressed ephrinA ligands on retinal ganglion cell axons. Neuron. 1999; 22:731–742. [PubMed: 10230793]

Howard MA, Rodenas-Ruano A, Henkemeyer M, Martin GK, Lonsbury-Martin BL, Liebl DJ. Eph receptor deficiencies lead to altered cochlear function. Hear Res. 2003; 178:118–130. [PubMed: 12684184]

Howell DM, Morgan WJ, Jarjour AA, Spirou GA, Berrebi AS, Kennedy TE, Mathers PH. Molecular guidance cues necessary for axon pathfinding from the ventral cochlear nucleus. J Comp Neurol. 2007; 504:533–549. [PubMed: 17701984]

Hsieh CY, Cramer KS. Deafferentation induces novel axonal projections in the auditory brainstem after hearing onset. J Comp Neurol. 2006; 497:589–599. [PubMed: 16739167]

Hsieh CY, Hong CT, Cramer KS. Deletion of EphA4 enhances deafferentation-induced ipsilateral sprouting in auditory brainstem projections. J Comp Neurol. 2007; 504:508–518. [PubMed: 17702003]

Hsieh CY, Nakamura PA, Luk SO, Miko IJ, Henkemeyer M, Cramer KS. Ephrin-B reverse signaling is required for formation of strictly contralateral auditory brainstem pathways. J Neurosci. 2010; 30:9840–9849. [PubMed: 20660266]

Jevince AR, Kadison SR, Pittman AJ, Chien CB, Kaprielian Z. Distribution of EphB receptors and ephrin-B1 in the developing vertebrate spinal cord. J Comp Neurol. 2006; 497:734–750. [PubMed: 16786562]

Kadison SR, Makinen T, Klein R, Henkemeyer M, Kaprielian Z. EphB receptors and ephrin-B3 regulate axon guidance at the ventral midline of the embryonic mouse spinal cord. J Neurosci. 2006; 26:8909–8914. [PubMed: 16943546]

Kil J, Kageyama GH, Semple MN, Kitzes LM. Development of ventral cochlear nucleus projections to the superior olivary complex in gerbil. J Comp Neurol. 1995; 353:317–340. [PubMed: 7751434]

Kitzes LM, Kageyama GH, Semple MN, Kil J. Development of ectopic projections from the ventral cochlear nucleus to the superior olivary complex induced by neonatal ablation of the contralateral cochlea. J Comp Neurol. 1995; 353:341–363. [PubMed: 7751435]

Kullander K, Croll SD, Zimmer M, Pan L, McClain J, Hughes V, Zabski S, DeChiara TM, Klein R, Yancopoulos GD, Gale NW. Ephrin-B3 is the midline barrier that prevents corticospinal tract axons from recrossing, allowing for unilateral motor control. Genes Dev. 2001; 15:877–888. [PubMed: 11297511]

Kullander K, Klein R. Mechanisms and functions of Eph and ephrin signalling. Nat Rev Mol Cell Biol. 2002; 3:475–486. [PubMed: 12094214]

Kuwabara N, DiCaprio RA, Zook JM. Afferents to the medial nucleus of the trapezoid body and their collateral projections. J Comp Neurol. 1991; 314:684–706. [PubMed: 1816271]

Migani P, Bartlett C, Dunlop S, Beazley L, Rodger J. Ephrin-B2 immunoreactivity distribution in adult mouse brain. Brain Res. 2007; 1182:60–72. [PubMed: 17945206]

Miko IJ, Henkemeyer M, Cramer KS. Auditory brainstem responses are impaired in EphA4 and ephrin-B2 deficient mice. Hear Res. 2008; 235:39–46. [PubMed: 17967521]

Miko IJ, Nakamura PA, Henkemeyer M, Cramer KS. Auditory brainstem neural activation patterns are altered in EphA4- and ephrin-B2-deficient mice. J Comp Neurol. 2007; 505:669–681. [PubMed: 17948875]

Mostafapour SP, Cochran SL, Del Puerto NM, Rubel EW. Patterns of cell death in mouse anteroventral cochlear nucleus neurons after unilateral cochlea removal. J Comp Neurol. 2000; 426:561–571. [PubMed: 11027399]

Nakamura PA, Cramer KS. Formation and maturation of the calyx of Held. Hear Res. 2010; 276:70–78. [PubMed: 21093567]

Petros TJ, Shrestha BR, Mason C. Specificity and sufficiency of EphB1 in driving the ipsilateral retinal projection. J Neurosci. 2009; 29:3463–3474. [PubMed: 19295152]

Renier N, Schonewille M, Giraudet F, Badura A, Tessier-Lavigne M, Avan P, De Zeeuw CI, Chedotal A. Genetic dissection of the function of hindbrain axonal commissures. PLoS Biol. 2010; 8 e1000325.

Rodriguez-Contreras A, van Hoeve JS, Habets RL, Locher H, Borst JG. Dynamic development of the calyx of Held synapse. Proc Natl Acad Sci U S A. 2008; 105:5603–5608. [PubMed: 18375766]

Russell FA, Moore DR. Afferent reorganisation within the superior olivary complex of the gerbil: development and induction by neonatal, unilateral cochlear removal. J Comp Neurol. 1995; 352:607–625. [PubMed: 7722003]

Rusu SI, Borst JG. Developmental changes in intrinsic excitability of principal neurons in the rat medial nucleus of the trapezoid body. Dev Neurobiol. 2011; 71:284–295. [PubMed: 21394932]

Sanes DH. An in vitro analysis of sound localization mechanisms in the gerbil lateral superior olive. J Neurosci. 1990; 10:3494–3506. [PubMed: 2172478]

Yokoyama N, Romero MI, Cowan CA, Galvan P, Helmbacher F, Charnay P, Parada LF, Henkemeyer M. Forward signaling mediated by ephrin-B3 prevents contralateral corticospinal axons from recrossing the spinal cord midline. Neuron. 2001; 29:85–97. [PubMed: 11182083]

Zimmer M, Palmer A, Kohler J, Klein R. EphB-ephrinB bi-directional endocytosis terminates adhesion allowing contact mediated repulsion. Nat Cell Biol. 2003; 5:869–878. [PubMed: 12973358]

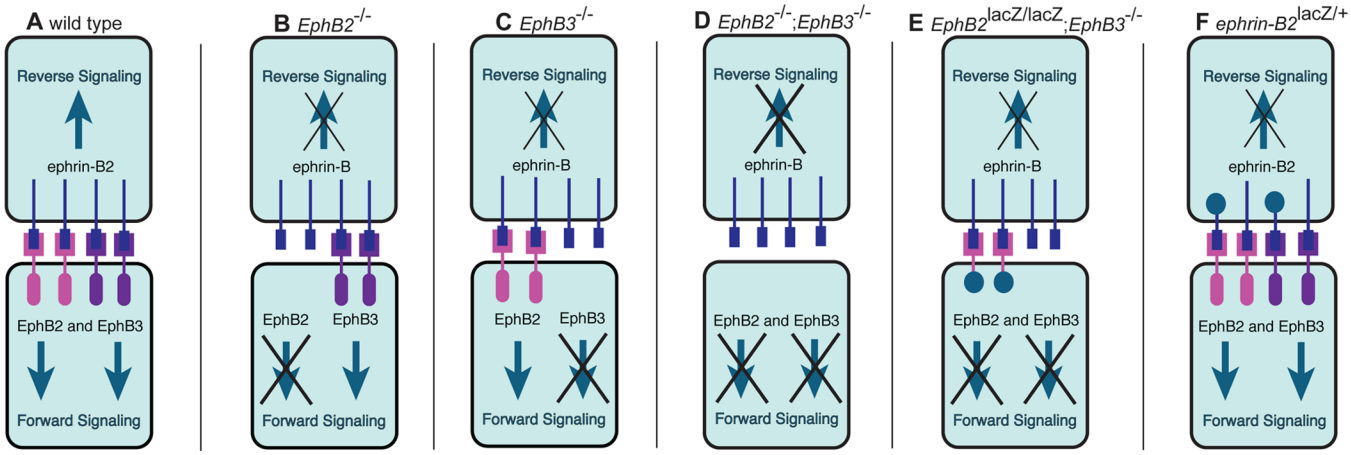

Figure 1.

Schematic of EphB signaling in wild type and mutant mice. In wild type mice, there is EphB2 and EphB3 forward signaling and ephrin-B2 reverse signaling (A). In *EphB2*$^{-/-}$ mice, there is no EphB2 forward signaling and no EphB2-elicited reverse signaling (B). *EphB3*$^{-/-}$ mice have no EphB3 forward signaling and no EphB3-elicited reverse signaling (C). *EphB2*$^{-/-}$;*EphB3*$^{-/-}$ double mutant mice have no forward signaling through EphB2 and EphB3 and no EphB2- and EphB3-elicited reverse signaling (D). In *EphB2*$^{lacZ/lacZ}$;*EphB3*$^{-/-}$ mice, there is no EphB2 forward signaling, no EphB3 forward or reverse signaling, but EphB2-elicited reverse signaling is intact (E). *Ephrin-B2*$^{lacZ/+}$ mice have intact ephrin-B2 forward signaling, but reduced ephrin-B2 reverse signaling (F).

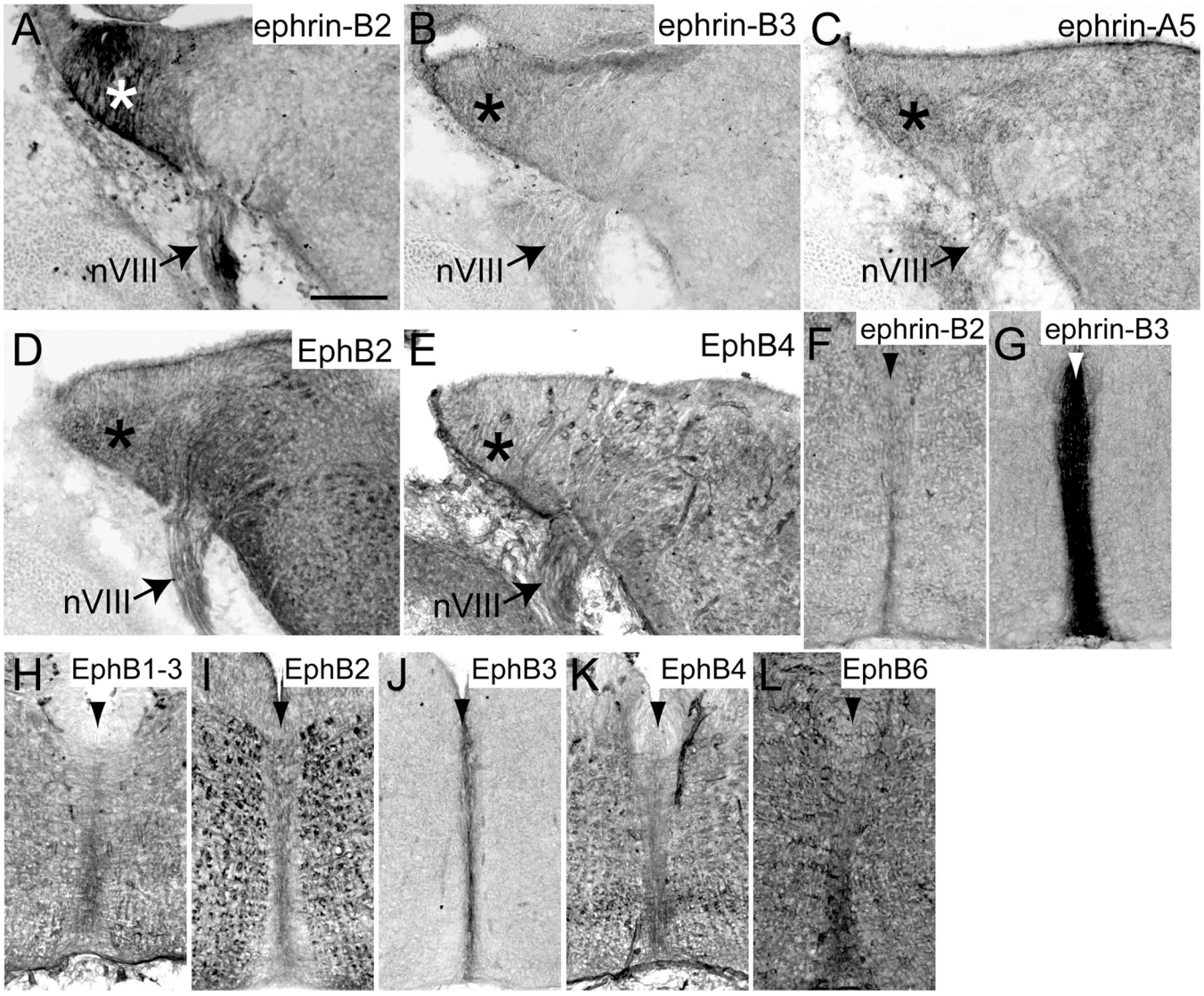

Figure 2.

EphB expression in coronal sections through the auditory brainstem at embryonic day 13.5. Ephrin-B2 (A), ephrin-B3 (B), ephrin-A5 (C), EphB2 (D), and EphB4 (E) are expressed in the cochlear nucleus (asterisks). Ephrin-B2 (F), ephrin-B3 (G), EphB1, 2, and 3 (H–J), EphB4 (K), and EphB6 (L) are expressed at the midline (arrowhead) of the brainstem. Scale bar in A represents 100 μm and applies to all panels.

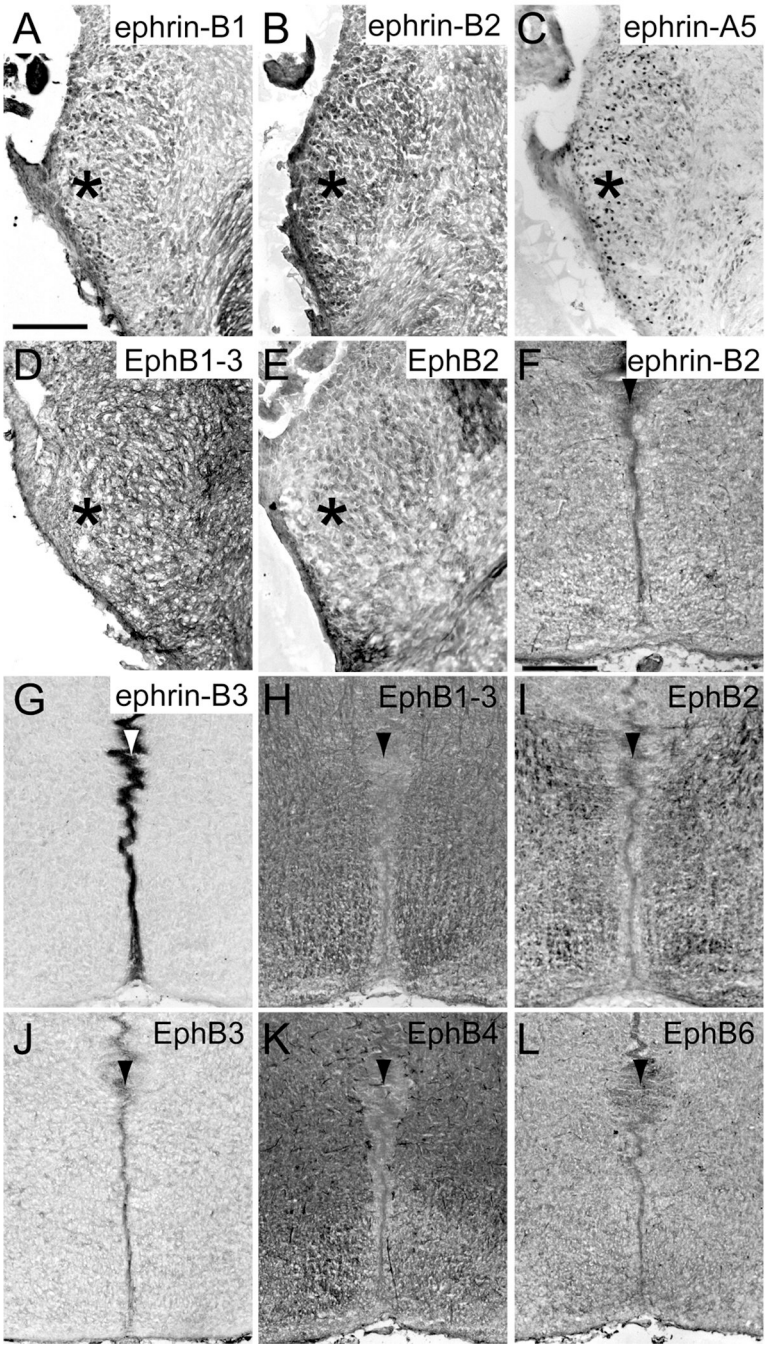

Figure 3.

EphB expression in coronal sections through the auditory brainstem at embryonic day 17.5. Ephrin-B1 (A), ephrin-B2 (B), ephrin-A5 (C), and EphB1, 2, and 3 (D–E) are expressed in the VCN (asterisks). Ephrin-B2 (F), ephrin-B3 (G), and all EphB receptors (H–L) are expressed at the midline (arrowhead) of the brainstem. Scale bar in A represents 100 μm and applies to panels A–E. Scale bar in F represents 200 μm and applies to panels F–L.

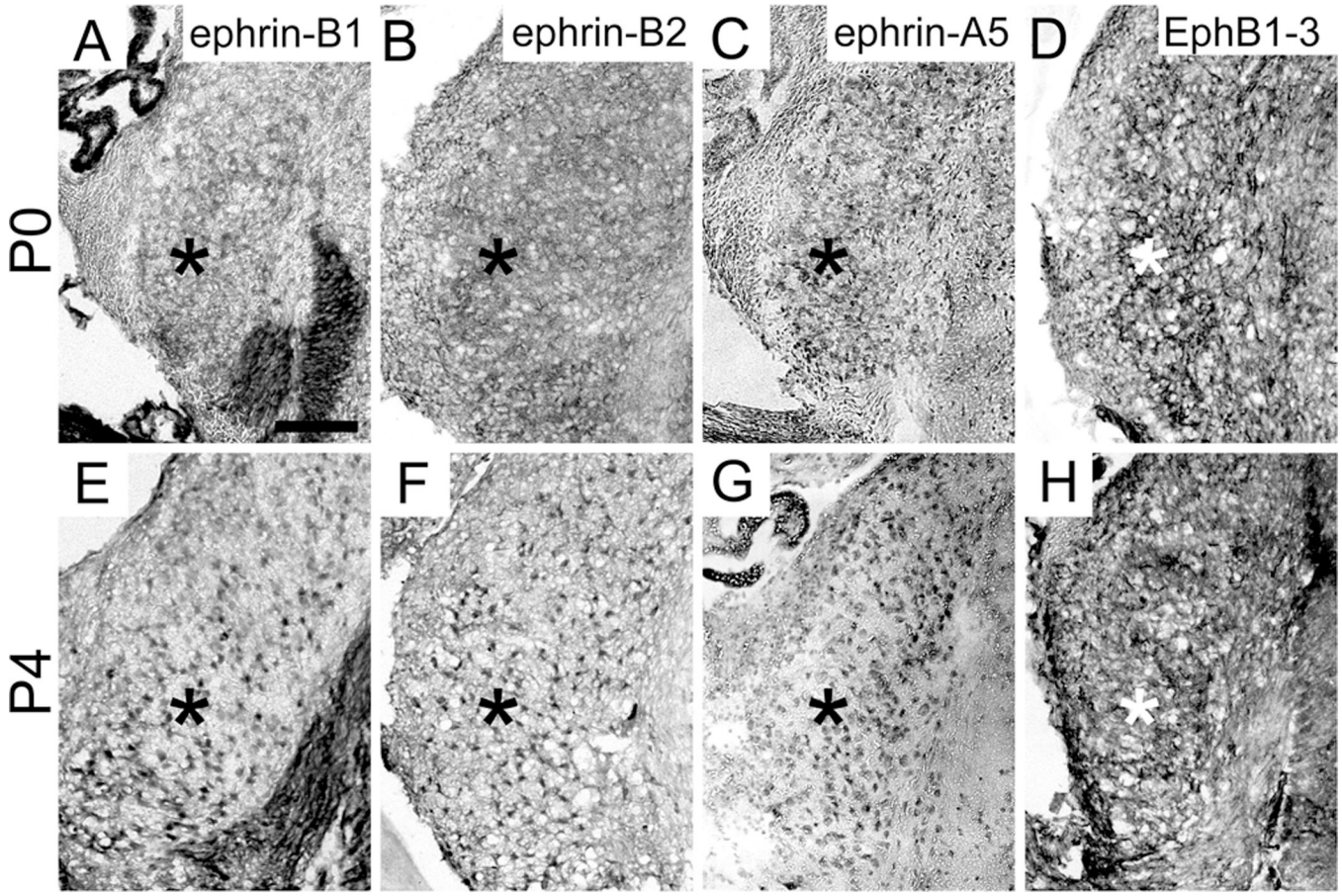

Figure 4.
EphB expression in the VCN at postnatal days 0 and 4. Ephrin-B1 (A), ephrin-B2 (B), ephrin-A5 (C), and EphB1-3 (D) are expressed in the VCN (asterisks) at P0 and at P4 (E–H, respectively). Scale bar in A represents 100 μm and applies to all panels.

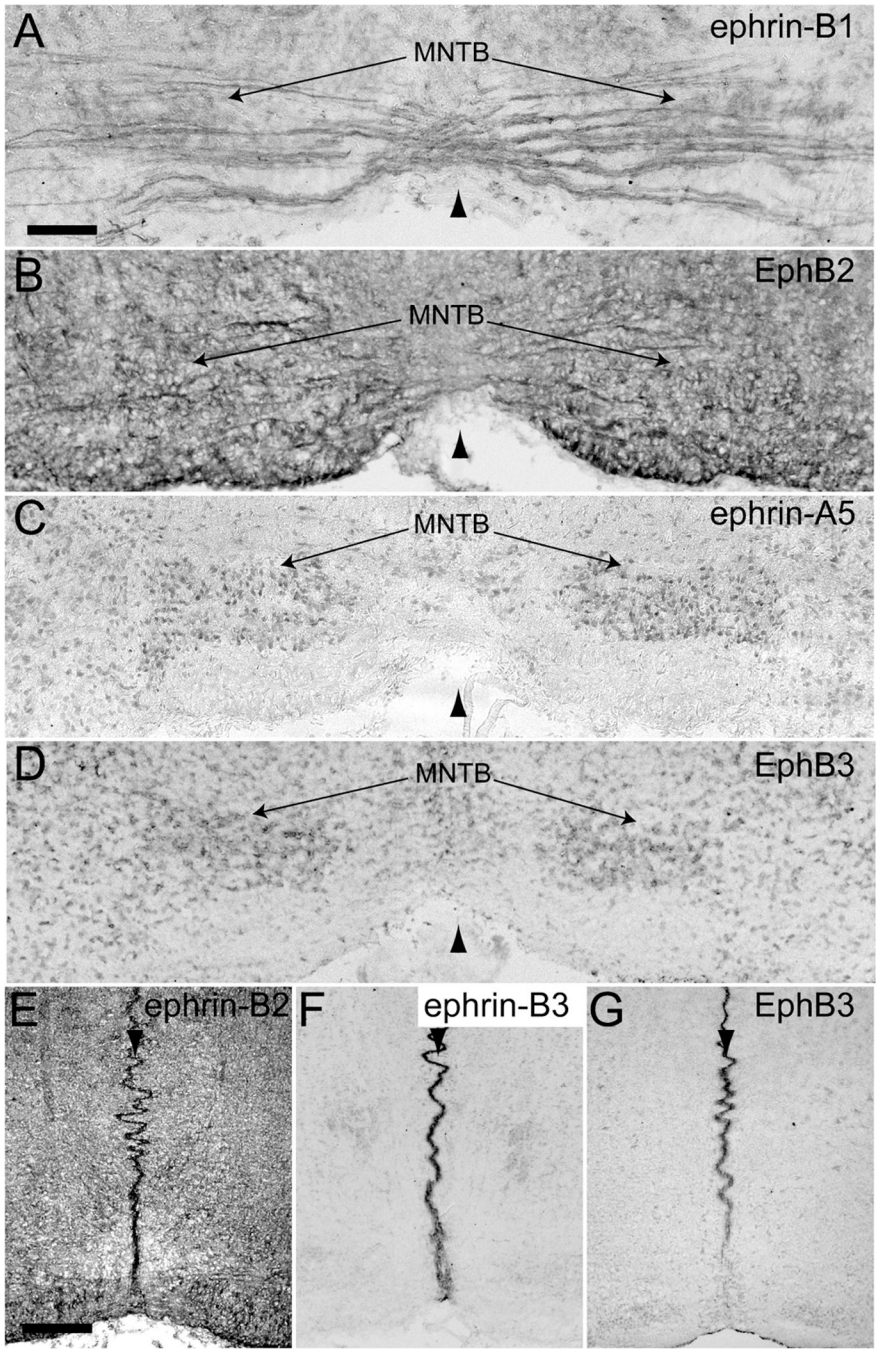

Figure 5.

EphB expression in coronal sections through the auditory brainstem at postnatal day 0. Ephrin-B1 (A) and EphB2 (B) are expressed in VCN axons. Ephrin-B1 (A), ephrin-A5 (C) and EphB3 (D) are expressed in MNTB. Ephrin-B2 (E), ephrin-B3 (F), and EphB3 (G) are expressed at the midline (arrowhead in all panels) of the brainstem. Scale bar in A represents 100 μm and applies to panels A–D. Scale bar in E represents 200 μm and applies to panels E–G.

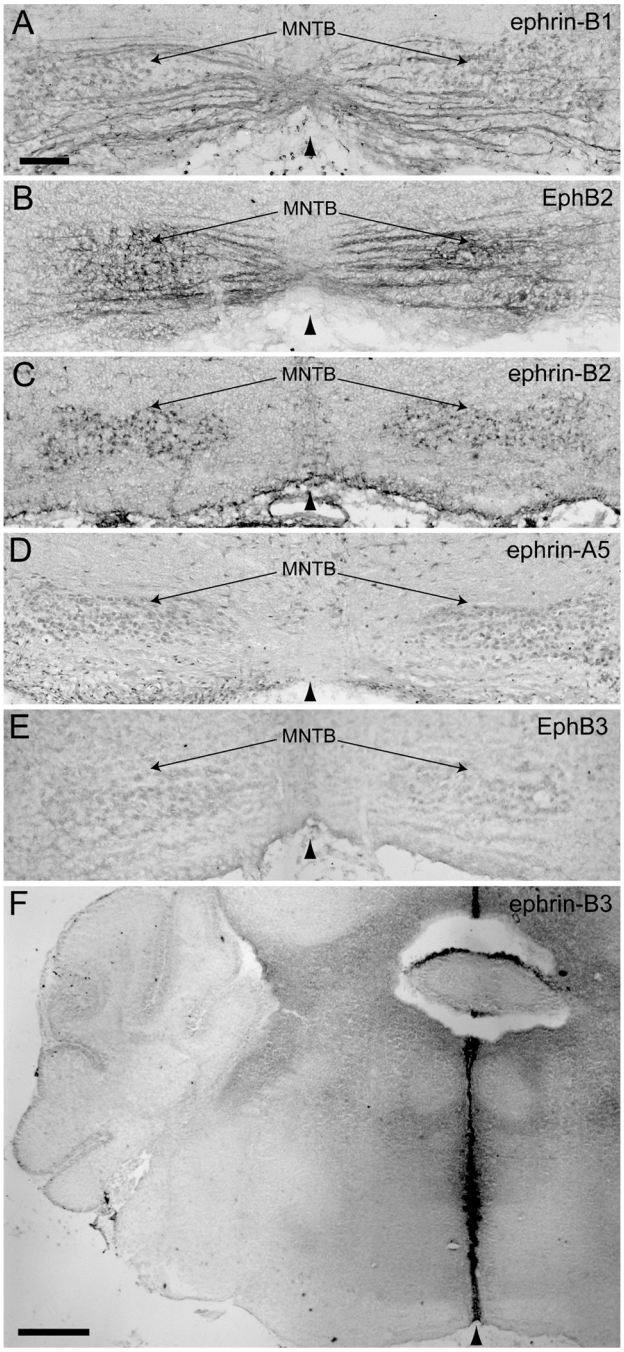

Figure 6.

EphB expression in coronal sections through the auditory brainstem at postnatal day 4–5. Ephrin-B1 (A) and EphB2 (B) are expressed in VCN axons. Ephrin-B1 (A), ephrin-B2 (C), ephrin-A5 (D), and EphB3 (E) are expressed in MNTB. Ephrin-B3 (F) is expressed at the midline (arrowhead in all panels) of the brainstem. Scale bar in A represents 100 μm and applies to panels A–E. Scale bar in F represents 400 μm and applies to that panel only.

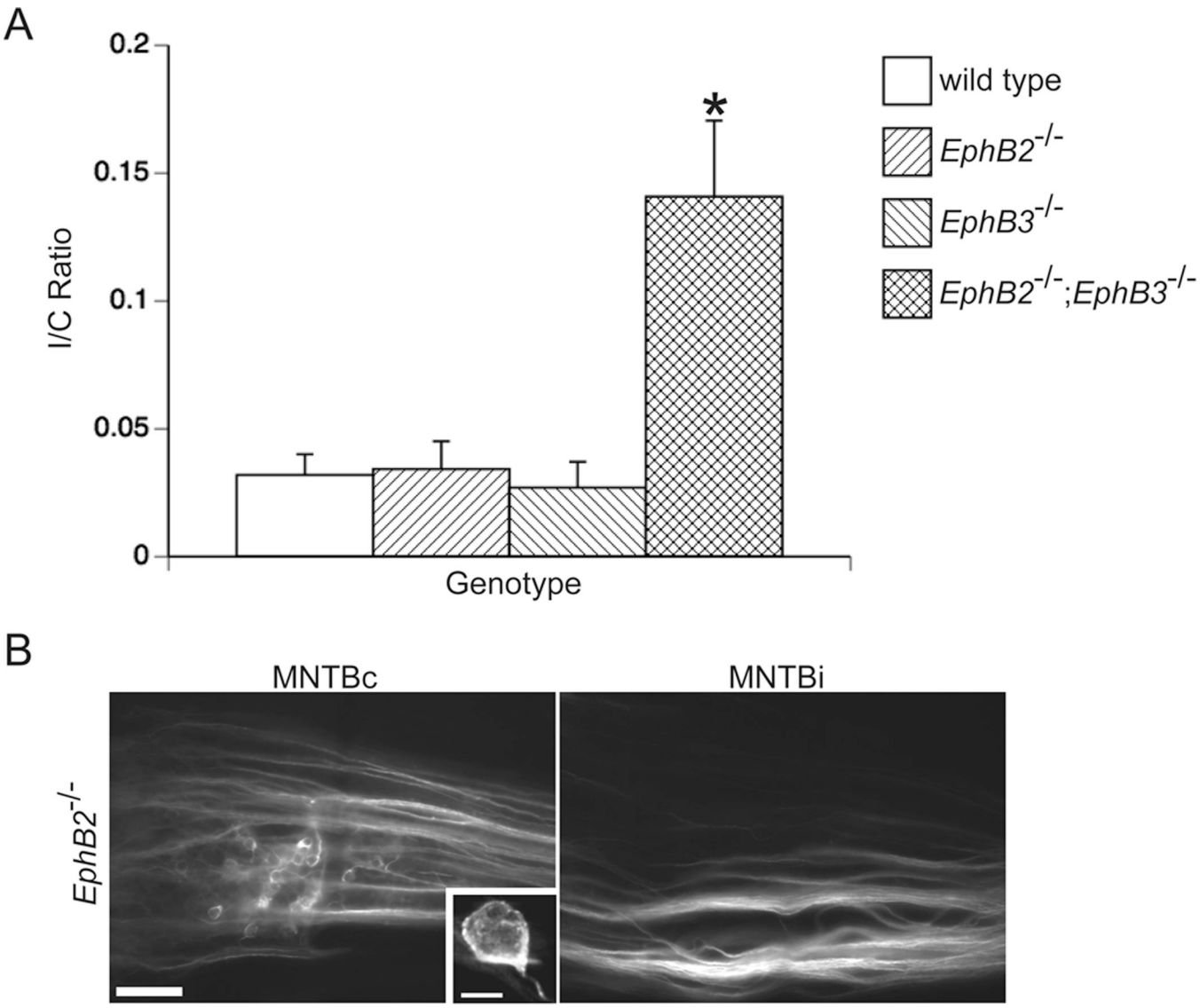

Figure 7.

EphB2 and EphB3 are necessary for the normal development of the VCN-MNTB projection. After dye placement into VCN on one side, labeled calyceal terminations were counted in the ipsilateral MNTB (MNTBi) and contralateral MNTB (MNTBc) to calculate an ipsilateral/contralateral (I/C) ratio in wild type, *EphB2*$^{-/-}$, *EphB3*$^{-/-}$, and *EphB2*$^{-/-}$;*EphB3*$^{-/-}$ mice. Null mutations in *EphB2* or *EphB3* alone do not phenocopy *EphB2*;*EphB3* double mutant mice, which have I/C ratios greater than wild type mice (A; $P < 0.05$, asterisk). Mean I/C ratios from *EphB2* and *EphB3* single mutant mice do not differ from the mean I/C ratio of wild type mice (A; $P > 0.05$). Projections from VCN are restricted to MNTBc in *EphB2*$^{-/-}$ mice, suggesting that ephrin-B reverse signaling is not elicited by EphB2 alone (B). A high-power image of a typical calyx of Held is shown in the inset of panel B. Scale bar in panel B represents 100 μm. Scale bar in the panel B inset represents 10 μm.

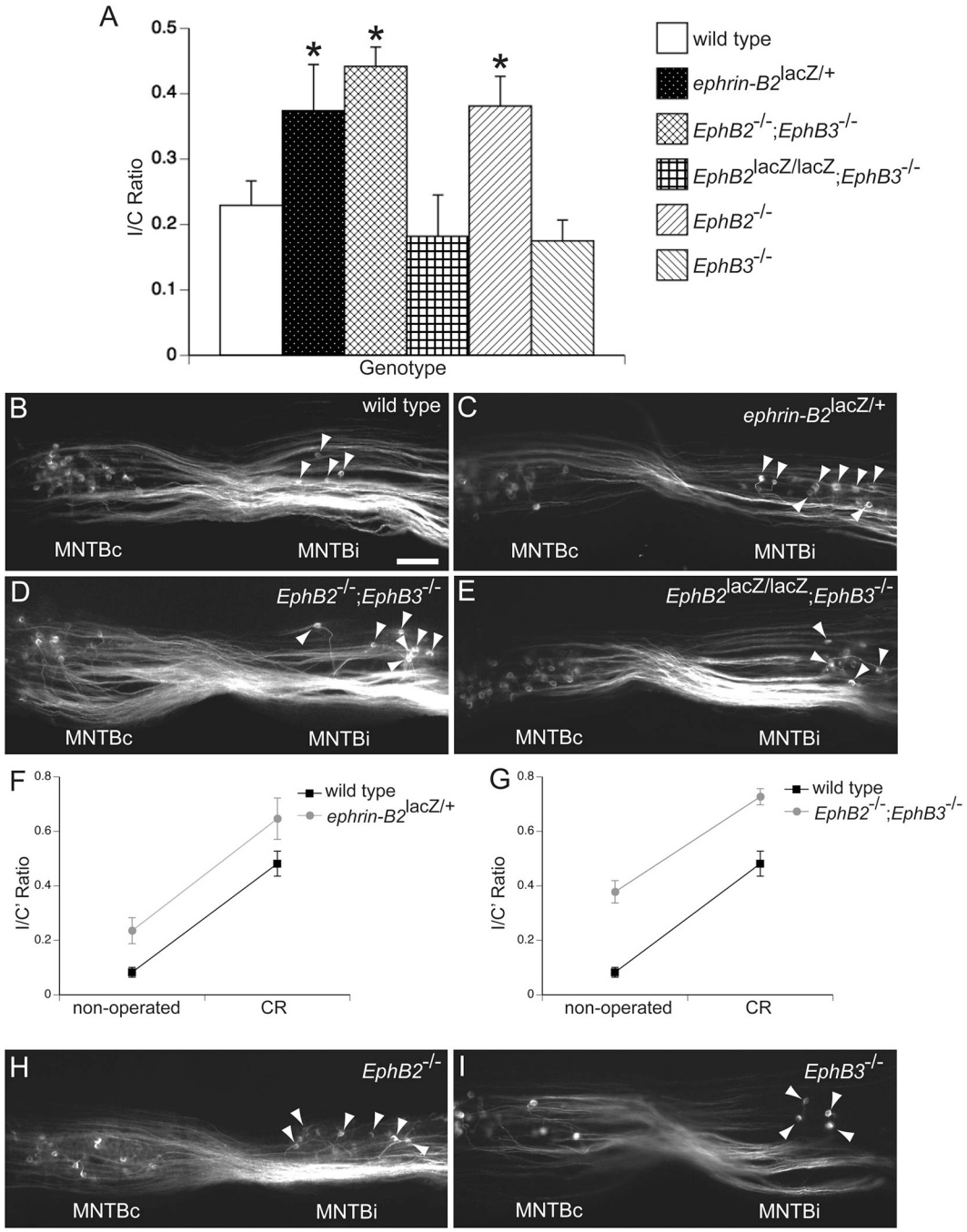

Figure 8.

EphB signaling regulates deafferentation-induced innervation of the ipsilateral MNTB. I/C ratios after unilateral cochlea removal (CR) at P2-3 were grouped by genotype (A). Asterisks indicate groups that have mean I/C ratios greater than the mean I/C ratio for wild type mice ($P < 0.05$). Examples of coronal sections after dye-labeling in unilaterally deafferented wild type (B), *ephrin-B2*$^{lacZ/+}$ (C), *EphB2*$^{-/-}$;*EphB3*$^{-/-}$ (D), and *EphB2*$^{lacZ/lacZ}$;*EphB3*$^{-/-}$ (E), demonstrate bilateral VCN-MNTB projections. Calyceal terminations in the ipsilateral MNTB (MNTBi) are indicated with arrowheads. Because non-operated *ephrin-B2*$^{lacZ/+}$ and *EphB2*$^{-/-}$;*EphB3*$^{-/-}$ mice have I/C ratios greater than non-operated wild type mice, we further analyzed the CR data from these two lines with a two-

way ANOVA on arcsine-transformed I/C ratios (I/C'). We found no significant genotype-surgical status interaction for both lines (F and G; $P > 0.05$). VCN-MNTB tracings in *EphB2*$^{-/-}$ (H) and *EphB3*$^{-/-}$ (I) single mutant mice demonstrate that the mean I/C ratio of operated *EphB2*$^{-/-}$, but not *EphB3*$^{-/-}$, mice was greater than the mean I/C ratio of operated wild type mice (A; $P < 0.05$). Scale bar in B represents 200 μm and applies to panels B–E and H–I.

Table 1

Summary of Eph protein expression in auditory regions and the midline at E13.5 to P4.

	VCN	VCN	MNTB	midline
ephrin-B1	E17.5, P0, P4	P0, P4	P0, P4	
ephrin-B2	E13.5, E17.5, P0, P4		P4	E13.5, E17.5, P0
ephrin-B3	E13.5			E13.5, E17.5, P0, P4
ephrin-A5	E13.5, E17.5, P0, P4		P0, P4	
EphB1-3	E17.5, P0, P4			E13.5, E17.5
EphB2	E13.5, E17.5, P0, P4	P0, P4		E13.5, E17.5
EphB3	E17.5, P0, P4		P0, P4	E13.5, E17.5, P0
EphB4	E13.5			E13.5, E17.5
EphB6				E13.5, E17.5